Effective Nonlinear Parameter Measurement Using FWM in Optical Fibers in a Low Power Regime

Nuno Alexandre Silva, Nelson Jesus Muga, and Armando Nolasco Pinto, *Senior Member, IEEE*

***Abstract*—The four-wave mixing (FWM) process in a low power regime is studied both theoretically and experimentally. The coupled-equations for the complex amplitudes are derived and solved. The proposed model is compared with experimental data. Results shows the need of considering both nonlinear and polarization dependent effects in order to obtain an accurate description of the four-wave mixing process in a low power regime. The effective nonlinear parameter is experimentally measured in a dispersion-shifted fiber, and the transition region between an almost co-polarized situation to a decorrelated state of polarization is observed.**

***Index Terms*—Nonlinear optics, optical fiber polarization, optical mixing.**

I. Introduction

FOUR-WAVE MIXING (FWM) occurs when light of two or more frequencies (known as pump and signal fields) are launched into a fiber, giving rise to a new frequency (known as idler). At the same time that the idler is generated the signal is amplified [1]. FWM is a nonlinear process, described by the third-order nonlinear susceptibility, $\chi^{(3)}$, and its origin is in the nonlinear response of bound electrons to an applied optical field [1].

FWM is a major source of nonlinear crosstalk in wavelength-division multiplexing lightwave systems [2]. Besides that, FWM can be used to implement fiber-optic parametric amplifiers [3]–[5], wavelength converters [4], [6]–[8] and single-photons and entangled photon-pairs sources [9]–[11].

In 1974, the phase-matched nonlinear mixing in a silica fiber was observed [12]. Since then, generalized studies of FWM in optical fibers taking into account Raman scattering and polarization effects have been carried out [13]–[17].

Most of the work related with FWM in optical fibers has been done around the zero-dispersion wavelength of the fiber [18]–[21], or with the pump and signal wavelengths placed very closely [22]. In these conditions the phase-matching is easily achieved and efficient FWM is obtained [18]–[22]. All these experiments were performed in a high power regime in order to enhance the FWM effect.

Manuscript received November 03, 2008; revised June 01, 2009 and August 17, 2009. Current version published December 31, 2009. This work was supported in part by the Instituto de Telecomunicações under the Laboratório Associado program supported by the Fundação para a Ciência e Tecnologia, FCT, and in part by the European Union FEDER program, through the IT/LA projects "Quantum" and "QuantTel."

N. A. Silva and N. J. Muga are with the Departamento de Física, Universidade de Aveiro and Instituto de Telecomunicações, 3810-193 Aveiro, Portugal (e-mail: nasilva@av.it.pt; muga@av.it.pt).

A. N. Pinto is with the Departamento de Electrónica, Telecomunicações e Informática, Universidade de Aveiro and Instituto de Telecomunicações, 3810-193 Aveiro, Portugal (e-mail: anp@ua.pt).

Color versions of one or more of the figures in this paper are available online at http://ieeexplore.ieee.org.

Digital Object Identifier 10.1109/JQE.2009.2032558

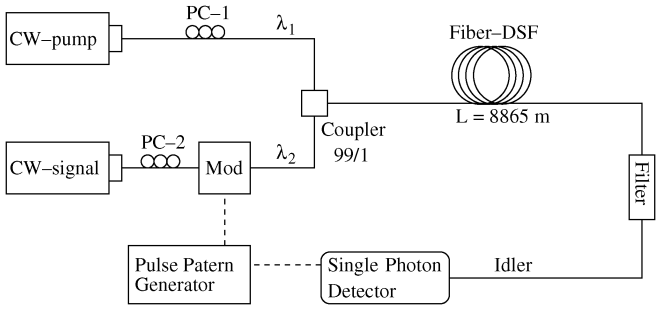

Fig. 1. Experimental arrangement for measuring the optical power generated through four-wave mixing in a low power regime. The dashed lines represents electrical signals and the solid lines the optical path. Details of the experiment are presented in the text.

Recently, FWM has been used in quantum optics experiments to generate single-photons and entangled photon-pairs [23]–[27]. Single-photons and entangled photon-pairs have been used for quantum cryptographic experiments, mainly quantum key distribution. When compared with others techniques for single-photons and entangled photon-pairs generation, FWM has the advantage of generating the photons already inside the optical fiber. In these experiments, FWM is obtained with very low pump powers [1], [9], [14]. Therefore, an accurate description of the FWM process in this low power regime is required in order to guide this new kind of experiments.

This paper contains four sections. In Section II, the experimental setup used to analyse the FWM process in a low power regime is described. In Section III, a new theoretical model to describe the FWM process in a low power regime is presented. We discuss the influence of the nonlinear contribution and polarization dependent effects in the efficiency of the FWM process. We also analyse the efficient generation of the idler wave outside the zero-dispersion of the fiber and with pump and signal far apart. All the theoretical results presented are confronted with experimental data, obtained for a dispersion-shifted fiber. In Section IV the main results presented in this paper are summarized.

II. Experimental Setup and the FWM Process

A schematic of our experimental setup is shown in Fig. 1. This setup was used to measure the optical power of the idler wave generated through the FWM process in a low power regime.

In the experimental setup, Fig. 1, a pump, λ_1 from a DFB laser source operating in a continuous mode passes through a polarization controller (PC-1) before being coupled to another optical

signal, λ_2 from a tunable laser source, that is modulated externally to produce optical pulses with a width at half maximum of approximately 1.6 ns and repetition rate of 610.3 kHz. The two optical fields are launched into a dispersion-shifted fiber (DSF), with incident powers $P_1(0)$ and $P_2(0)$ for pump and signal fields, respectively. The DSF has a dispersion slope at zero-dispersion wavelength $dD_c/d\lambda = 0.069\ \mathrm{ps/nm^2 - km}$, length $L = 8865\ \mathrm{m}$, zero-dispersion wavelength $\lambda_0 = 1547.34$ nm, attenuation $\alpha_{dB/km} = 0.2\ \mathrm{dB/km}$ and nonlinear coefficient $\gamma = 2.36\ \mathrm{W^{-1}km^{-1}}$. The zero-dispersion wavelength and the dispersion slope of the fiber were measured with an *Optical Network Analyzer, 86038-90B01*, from Agilent. At the fiber output, a filter blocks the pump and signal waves. The idler wave, $\lambda_3 = \lambda_1\lambda_2/(2\lambda_2 - \lambda_1)$ [1], [22], passes through the filter and reaches a single-photon detector. The single-photon detector is based on an APD, operating in the so-called Geiger mode, being $T_g = 2.5$ ns the time during which the gate of the detector is open. The detector quantum efficiency is $\eta_{det} = 10\%$ and the dark count probability per gate is $Pr_{dc} = 5\times10^{-5}$ [28]. The Noise Equivalent Power of the detector is $\mathrm{NEQ} \approx 2.56\times10^{-16}\ \mathrm{W}/\sqrt{\mathrm{Hz}}$, and the probability of having a count when a single-photon reaches the detector compared with the probability of having a count due to the dark counts is $Pr_{\mathrm{eff}} = 5 \times 10^{-4}$ [29]. The optical power of the idler wave can be obtained from the average number of photons per pulse that arrive to the single-photon detector using

$$P_m = \frac{\langle n\rangle hc}{\lambda_3 T_g} 10^{\alpha_d/10} \tag{1}$$

where P_m represents the measured idler power at the exit of the fiber, $\langle n\rangle$ is the average number of idler photons per pulse that arrive to the single-photon detector, h is the Planck constant, c is the speed of light in vacuum and α_d is the attenuation, in decibels, from the fiber output to the detector. From (1) with $\alpha_d = 0$ and with $\langle n\rangle$ replaced by $n \equiv 1$ we obtain the minimum measurable power of the detector, $P_m \approx 5 \times 10^{-11}$ W. In our experiment we perform the estimation of $\langle n\rangle$ using a measurement period of 20 s. The average number of idler photons that reaches to the single-photon detector is given by [30], [31]

$$\langle n\rangle = \frac{1}{\eta_{det}} \ln\left(\frac{Pr_{dc} - 1}{Pr_{av} - 1}\right) \tag{2}$$

where Pr_{av} is the probability of avalanche per gate.

The FWM process in optical fibers was investigated, theoretically and experimentally, by Hill *et al.* [32], and their work was latter reformulated by Shibata *et al.* [33] to include the dependence of the phase-matching. According with [18], [22], [33], the optical power evolution of the idler wave in the single pump case can be described by

$$P_3(z) = \left(\gamma P_1(0) z_{\mathrm{eff}}\right)^2 P_2(0) \exp\{-\alpha z\}\eta \tag{3}$$

with

$$z_{\mathrm{eff}} = \frac{1 - \exp\{-\alpha z\}}{\alpha} \tag{4}$$

where α is the fiber losses, and η is the efficiency of the process given by

$$\eta = \frac{\alpha^2}{\alpha^2 + (\Delta\beta)^2}\left(1 + \frac{4\exp\{-\alpha z\}\sin^2(\Delta\beta z/2)}{\left(1 - \exp\{-\alpha z\}\right)^2}\right) \tag{5}$$

and $\Delta\beta$ is the phase-matching condition

$$\Delta\beta = -\frac{2\pi c\lambda_0^3}{\lambda_1^3\lambda_2^2}\frac{dD_c}{d\lambda}\bigg|_{\lambda_0}(\lambda_1 - \lambda_0)(\lambda_1 - \lambda_2)^2. \tag{6}$$

III. FWM in a Low Power Regime

In this section we present a new theoretical description of the FWM process in a low power regime, in order to obtain a very low number of created photons in the idler wave. In Section III-A, we derive and solve the coupled-equations for the electrical field complex amplitudes. In Section III-B, we analyse the polarization effects in the optical power evolution of the idler wave.

A. Nonlinear Contribution

We assume that all fields involved in the FWM process (pump, signal and idler) remain co-polarized along the propagation in the fiber, and in order to avoid multiple FWM processes in the optical fiber [34]–[36], the pump and signal powers are maintained in a low power regime. Under the slowly varying envelope approximation, the evolution of the electrical field complex amplitudes inside an optical fibers (A_1 for pump, A_2 for signal and A_3 for idler) are governed by the nonlinear Schrödinger equation [1]

$$\frac{\partial A}{\partial z} + \frac{\alpha}{2}A = \sum_{m=0}^{+\infty}\frac{i^{m+1}\beta_m}{m!}\frac{\partial^m A}{\partial t^m} + i\gamma\left[1 + \frac{i}{\omega_0}\frac{\partial}{\partial t}\right]P^{NL}(z,t) \tag{7}$$

where β_m is the m^{th} order dispersion coefficient and $P^{NL}(z,t)$ is the third-order nonlinear polarization given by

$$P^{NL}(z,t) = A(z,t)\int_{-\infty}^{+\infty} R(\tau)\left|A(z,t-\tau)\right|^2 d\tau \tag{8}$$

where $R(\tau)$ is the fiber nonlinear response function [1].

Equation (7) is quite general in the sense that it includes the effects of group-velocity dispersion, attenuation, self-phase modulation, cross-phase modulation, stimulated Raman scattering and FWM process.

Equation (7) does not have an analytical solution. However, with some considerations an approximated analytical solution can be obtained. Assuming that each field component is not time dependent (CW condition), that $|A_1|^2 \gg |A_{2,3}|^2$, undepleted-pump approximation [1], and instantaneous nonlinear response [1], we obtain

$$\frac{\partial A_1(z)}{\partial z} + \frac{\alpha}{2}A_1(z) \approx i\gamma A_1(z)P_1(z) \tag{9a}$$

$$\frac{\partial A_2(z)}{\partial z} + \frac{\alpha}{2}A_2(z) \approx i\gamma\left[2A_2(z)P_1(z) + A_1^2(z)A_3^*(z)e^{-i\Delta\beta z}\right] \tag{9b}$$

$$\frac{\partial A_3(z)}{\partial z} + \frac{\alpha}{2}A_3(z) \approx i\gamma\left[2A_3(z)P_1(z) + A_1^2(z)A_2^*(z)e^{-i\Delta\beta z}\right] \tag{9c}$$

where

$$\Delta\beta = \beta(\omega_2) + \beta(\omega_3) - 2\beta(\omega_1). \tag{10}$$

Equation (9a) has an analytical solution

$$A_1(z) = A_1(0)\exp\{i\phi(z)\}\exp\{-\alpha z/2\} \tag{11}$$

where $P_1(0) = |A_1(0)|^2$ is the incident pump power, and

$$\phi(z) = \int_0^z \gamma P_1(z')dz' = \gamma P_1(0)\frac{1-\exp\{-\alpha z\}}{\alpha} \tag{12}$$

is the nonlinear phase shift caused by the Kerr effect [37]. By introducing the substitutions [37]

$$A_2(z) = A_s(z)\exp\left[i\left(\phi(z) - \frac{\Delta\beta}{2}z\right) - \frac{\alpha}{2}z\right] \tag{13a}$$

$$A_3(z) = A_i(z)\exp\left[i\left(\phi(z) - \frac{\Delta\beta}{2}z\right) - \frac{\alpha}{2}z\right] \tag{13b}$$

and assuming that only the signal and pump waves are incident at the fiber input, and considering $\alpha = 0$, the signal and idler waves at distance z are given by

$$A_s(z) = A_s(0)\left(\cos(\kappa z) + \frac{i}{\kappa}\left[\frac{\Delta\beta}{2} + \gamma P_1(0)\right]\sin(\kappa z)\right) \tag{14}$$

and

$$A_i(z) = i\gamma P_1(0)A_s^*(0)\frac{\sin(\kappa z)}{\kappa}. \tag{15}$$

In (14) and (15) the parametric gain, κ, is given by

$$\kappa = \sqrt{\frac{\Delta\beta}{2}\left(\frac{\Delta\beta}{2} + 2\gamma P_1(0)\right)}. \tag{16}$$

The effect of fiber losses is taken into account by replacing $P_1(0)$ in the solutions (14) and (15) with $P_1(0)z_{\text{eff}}/z$, valid for low-loss fibers [37]. In this regime the parametric gain is written as

$$\kappa = \sqrt{\frac{\Delta\beta}{2}\left(\frac{\Delta\beta}{2} + 2\gamma P_1(0)z_{\text{eff}}/z\right)} \tag{17}$$

where contributions from the phase-matching condition $\Delta\beta$ and nonlinear effects, given by $\gamma P_1(0)$ are included. If κ is real, the optical power of the idler wave can be express as

$$P_3(z) = (\gamma P_1(0)z_{\text{eff}})^2 P_2(0)\left|\frac{\sin(\kappa z)}{\kappa z}\right|^2 \exp\{-\alpha z\}. \tag{18}$$

From (6) and (17), κ is real for $\lambda_1 < \lambda_0$, or if $\lambda_1 > \lambda_0$ and

$$\frac{\Delta\beta}{2} + 2\gamma P_1(0)z_{\text{eff}}/z < 0. \tag{19}$$

However, the parametric gain κ becomes imaginary if $\lambda_1 > \lambda_0$ and [25]

$$\frac{\Delta\beta}{2} + 2\gamma P_1(0)z_{\text{eff}}/z > 0. \tag{20}$$

In that regime the parametric gain is written as

$$\kappa = i\sqrt{-\frac{\Delta\beta}{2}\left(\frac{\Delta\beta}{2} + 2\gamma P_1(0)z_{\text{eff}}/z\right)} \tag{21}$$

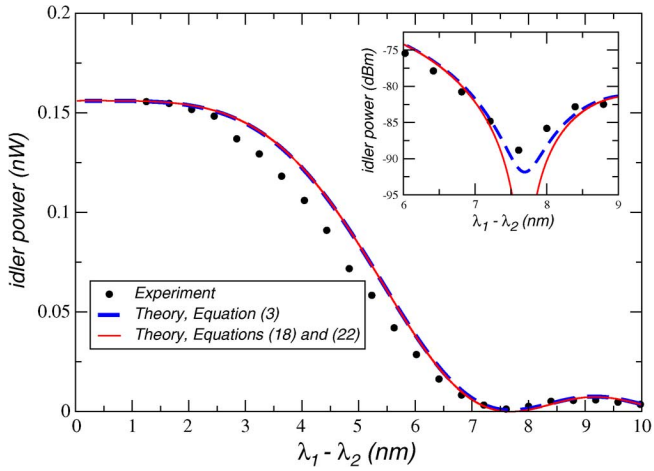

Fig. 2. Optical power of idler wave as a function of wavelength separation between pump and signal fields.The circles represents the measured optical power, the dashed line represents the theoretical model given by (3) and the solid line represents the theoretical model given by (18). Incident pump and signal powers are $P_1(0) = 8.71$ mW and $P_2(0) = 3.73 \times 10^{-3}$ mW, respectively, and the pump wavelength is $\lambda_1 = 1547.57$ nm.

and the optical power is expressed as

$$P_3(z) = (\gamma P_1(0)z_{\text{eff}})^2 P_2(0)\left|\frac{\sinh(\kappa z)}{\kappa z}\right|^2 \exp\{-\alpha z\}. \tag{22}$$

If fiber losses are neglected, (18) and (22) are equivalent to results presented in [1], [4], [38].

Comparing (3) with (18), the efficiency of the FWM process is now given by $\eta = |\sin(\kappa z)/\kappa z|^2$ and it is dependent of the nonlinear contribution $\gamma P_1(0)$. For high values of the nonlinear contribution (3) and (18) produce different results.

In Fig. 2 we plot the measured optical power and the theoretical predictions given by (3), (18) and (22) for the idler wave as a function of wavelength separation between pump and signal fields. From Fig. 2 we can see that for $2.8\text{ nm} < \lambda_1 - \lambda_2 < 5\text{ nm}$ the theoretical models and the experimental data does not coincide. That difference is analysed in Section III-B.

From (18) and (22) if $\lambda_1 = \lambda_0$ or if $\lambda_1 = \lambda_2$ the phase-matching condition becomes null (consequently $\kappa = 0$), and the optical power of the idler wave is maximum. However, efficient generation of idler wave can be achieved even when $\Delta\beta \neq 0$, making $\kappa = 0$. That particular case of interest occurs when the incident pump power is sufficiently strong so that

$$P_1(0) = -\frac{\Delta\beta}{4\gamma}\frac{z}{z_{\text{eff}}} \tag{23}$$

and the system is operating in the anomalous-dispersion regime, $\lambda_1 > \lambda_0$. In this case, although $\lambda_1 \neq \lambda_0$ the optical power of the idler wave grows as if $\lambda_1 = \lambda_0$.

In Fig. 3 we plot the optical power of the idler wave as a function of the pump power when $\lambda_1 = \lambda_0$, for two fixed values of the signal wavelength: $\lambda_2 = 1544.725$ nm and $\lambda_2 = 1545.322$ nm. We see from Fig. 3 that the idler power varies with the pump power quadratically (for the two distinct values of λ_2). This is expected from the theory, according with (3) and (18), when $\Delta\beta = 0$. We can also see that the idler power is almost independent of the signal wavelength. The fluctuations of the

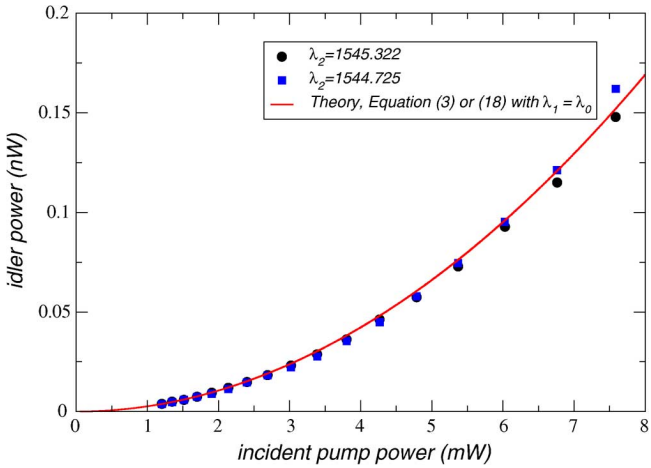

Fig. 3. Optical power of idler wave as a function of incident pump power, in the zero-dispersion wavelength of the fiber. The circles and the squares represents the measured optical power and the line represents the theoretical model given by (3) or (18) with $\lambda_1 = \lambda_0$. The input signal power used was $P_2(0) = 4.81 \times 10^{-3}$ mW.

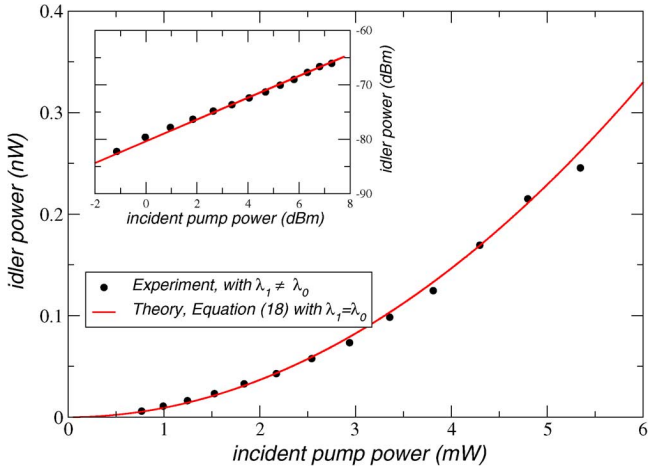

Fig. 4. Representation of the measured optical power of the idler field as a function of incident pump power for $\lambda_1 = 1547.37$ nm. The line represents the theoretical model given by (18) when $\lambda_1 = \lambda_0$. The incident signal power used was $P_2(0) = 1.67 \times 10^{-2}$ mW and the signal wavelength varies between 1543.532 nm and 1545.92 nm. The experimental incident pump power was adjusted according with (23).

zero-dispersion wavelength along the fiber length can influence the FWM process [18], [39], [40]. However, fluctuations with short coherence length, $\gamma P_1(0) L_c \ll 1$ (where L_c is the length over which the fluctuations occurs), and narrow wavelength separations, can be neglected. [39], [40]. Even if we assume that $L_c \approx L$, we obtain in our case $\gamma P_1(0) L_c \approx 0.18$. Considering the good agreement between the theoretical predictions and the experimental data present in Fig. 3, we assume that the fluctuations of the fiber zero-dispersion has almost no impact in our experiment.

In Fig. 4 we analyse the possibility of efficient generation of the idler wave inside an optical fiber outside the zero-dispersion of the fiber and with pump and signal far apart. Fig. 4 shows the measured optical power for $\lambda_1 \neq \lambda_0$ with the incident pump power given by (23) and the theoretical model given by (18) with $\lambda_1 = \lambda_0$ for the idler wave as a function of incident pump power.

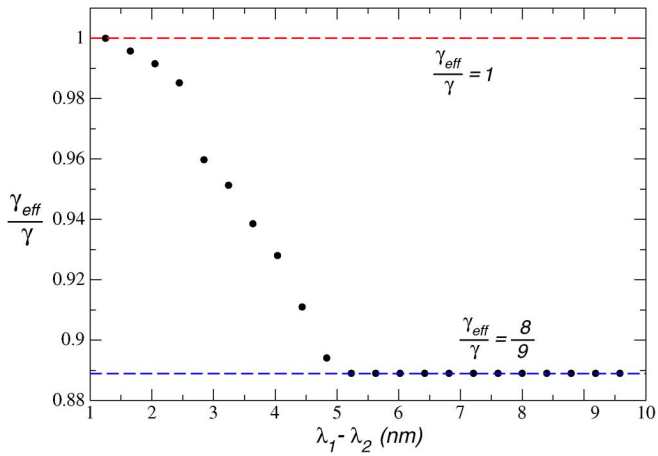

Fig. 5. Representation of the γ_{eff} variation with the wavelength separation between pump and signal fields. The data presented in the figure is obtained by fitting the experimental data presented in Fig. 2 to (18) and (22), with γ replaced by γ_{eff}.

The experimental results show a good agreement with theoretical predictions. This means that the generation of the idler field becomes the same as for the case when the pump wavelength is in the zero-dispersion wavelength of the fiber or when the signal and pump wavelengths are placed very closely. The explanation of this result is only possible due to the inclusion of the nonlinear contribution in the parametric gain.

B. Polarization Effects

The efficiency of the FWM process is dependent of the relative polarization of pump and signal fields [1]. The best efficiency is obtained when pump and signal are co-polarized, whereas the orthogonal scheme leads to the worst efficiency [1]. When pump and signal are orthogonal the optical power of the idler wave is about 1/9 of the power obtained with the co-polarized scheme [1], [14].

In the results presented in Fig. 2, we can see that with the increase of the wavelength separation between pump and signal, the idler power measured experimentally is smaller than the theoretical predictions. In the theoretical model it was assumed that all fields remain co-polarized along the propagation in the fiber. However, when the wavelength separation between pump and signal is increased the fields go from an almost co-polarized situation to a decorrelated state of polarization (SOP). The loss of efficiency in the FWM process due to the polarization decorrelation can be seen as a reduction of the value of the nonlinear parameter γ [41]–[45]. This can be described through a new parameter called effective nonlinear parameter γ_{eff}, which is dependent of the wavelength separation between pump and signal fields. If the nonlinear parameter present in (18) and (22) is replaced by the effective nonlinear parameter, γ_{eff}, the loss of efficiency in the generation of idler wave due to polarization effects can also be described by these two equations.

It can be seen in Fig. 5 the variation of the effective nonlinear parameter with the wavelength separation between pump and signal fields. The points represented in Fig. 5 were obtained by fitting the experimental data present in Fig. 2 to (18)

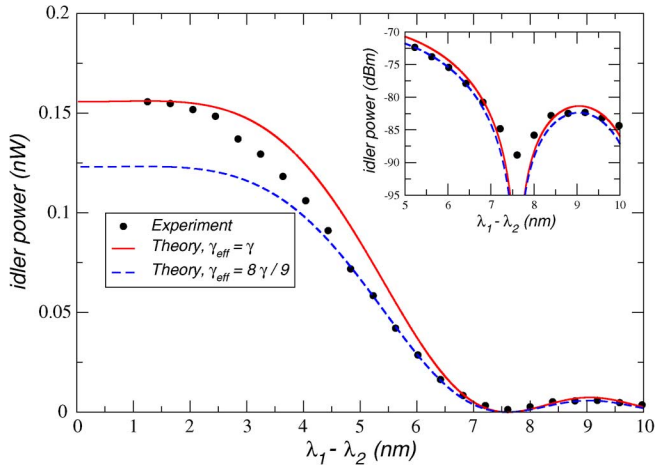

Fig. 6. Measured optical power of the idler wave as a function of $\lambda_1 - \lambda_2$. The solid and the dashed lines represents (18) and (22) with $\gamma_{\text{eff}} = \gamma$ and with $\gamma_{\text{eff}} = 8\gamma/9$, respectively.

and (22), with γ replaced by γ_{eff}. The results show that the effective nonlinear parameter is approximately equals to γ for $\lambda_1 - \lambda_2 < 2.8$ nm. However, with the increasing separation between pump and signal fields, the value of γ_{eff} rapidly decreases to $8\gamma/9$, and remains constant for $\lambda_1 - \lambda_2 > 5$ nm. This value for the effective nonlinear parameter is in agreement with theoretical predictions for polarization dependent processes in a strong mode coupling [41]–[45].

In Fig. 6 we present the theoretical model given by (18) and (22) for two values of γ_{eff}, γ and $8\gamma/9$, and the measured optical power for the idler wave as a function of wavelength separation between pump and signal. The comparison, between the two plots in Fig. 6, shows that the polarization effects decrease the idler power approximately by 1 dB, due to the reduction of γ_{eff}. The results also show that, until $\lambda_1 - \lambda_2 < 2.8$ nm the experimental data and theoretical prediction with $\gamma_{\text{eff}} = \gamma$ present a quasi-perfectly match. That means that for small wavelengths detunings the pump and signal fields remain approximately co-polarized along the optical fiber.

According with the theory of the principal states of polarization (PSP) [46], [47], exist a small frequency range over which the polarization mode dispersion vector is reasonably constant

$$\Delta\omega_{\text{psp}} \approx \frac{\pi}{4\langle\Delta\tau\rangle} \tag{24}$$

where $\langle\Delta\tau\rangle$ is the mean differential group delay (DGD). To evaluate the mean DGD we perform an experiment with the *Optical Network Analyzer*, and we find that $\langle\Delta\tau\rangle \simeq 0.362$ ps. For this value of mean DGD, the frequency range over which the SOP is reasonably constant is, $\Delta\omega_{\text{psp}} \simeq 2.17$ GHz. In terms of wavelength, the bandwidth is $\Delta\lambda_{\text{psp}} \simeq 2.75$ nm, which is in line with the value mentioned above, $\lambda_1 - \lambda_2 < 2.8$ nm. For $\lambda_1 - \lambda_2 > 5$ nm the experimental data is correctly describe with $\gamma_{\text{eff}} = 8\gamma/9$, which indicates that the pump and signal polarizations are mostly decorrelated.

The comparison between the results presented in Fig. 6 also show that exist a transition region, $2.8\text{ nm} < \lambda_1 - \lambda_2 < 5$ nm, over which the optical power evolution of the idler wave with the wavelength separation between pump and signal fields is

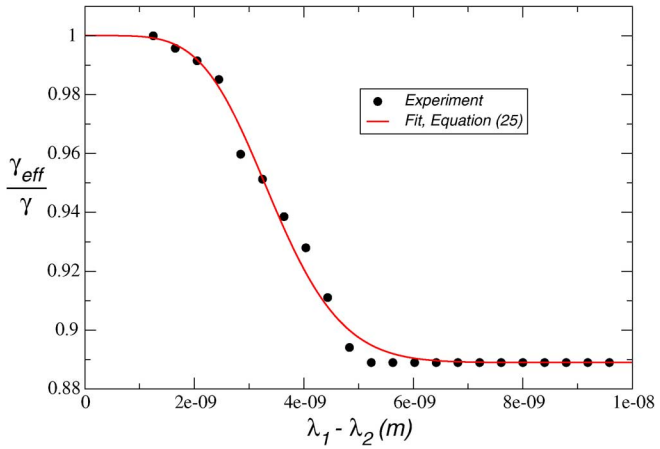

Fig. 7. Comparison between the points obtained for the γ_{eff} parameter, Fig. 5, and the fit with the hyperbolic secant function (25).

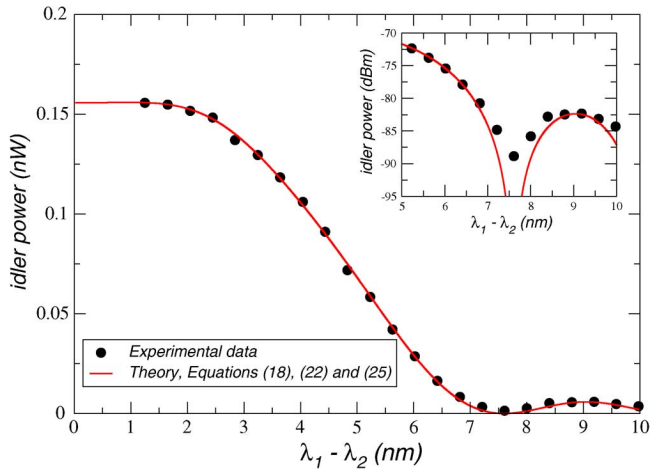

Fig. 8. Comparison between the experimental data for the idler power and theoretical model, equation (18) and (22) with $\gamma_{\text{eff}}(\Delta\lambda)$ given by (25). The theoretical model and the experimental data shows good agreement. The experimental parameters used are the same as the ones used to obtain Fig. 2.

not described by $\gamma_{\text{eff}} = \gamma$ or by $\gamma_{\text{eff}} = 8\gamma/9$. In that region the optical fields go from an almost co-polarized situation to a decorrelated state of polarization.

In order to describe analytically the γ_{eff} variation with the wavelength separation between pump and signal, we fit the result present in Fig. 5 with an hyperbolic secant function given by

$$\gamma_{\text{eff}}(\Delta\lambda) = \frac{8\gamma}{9} + \frac{\gamma}{9}\text{sech}\left(\frac{(\Delta\lambda)^{A_0}}{T_0}\right) \tag{25}$$

where A_0 and T_0 are the fitting parameters, and $\Delta\lambda = \lambda_1 - \lambda_2$. In Fig. 7 we represent the analytical equation for γ_{eff} with $A_0 \approx 2.15$ and $T_0 \approx 5.47826 \times 10^{-19}$, and the experimental data as a function of wavelength separation between pump and signal. The results presented in Fig. 7 show that the hyperbolic secant describes correctly the variation of the $\gamma_{\text{eff}}(\Delta\lambda)$ parameter with wavelength separation between pump and signal fields in the transition region $2.8\text{ nm} < \lambda_1 - \lambda_2 < 5$ nm.

Finally, in Fig. 8 we represent the measured optical power and the theoretical model for the idler wave as a function of wavelength separation between pump and signal.

The results presented in Fig. 8 shows a good agreement between the experimental data and the theoretical model given by (18) and (22) with $\gamma_{\text{eff}}(\Delta\lambda)$ given by (25).

IV. Conclusion

In summary, we investigated, both theoretically and experimentally, the FWM process in optical fibers in a low power regime. Using the coupled-equations, we derived a simple equation that governs the evolution of idler wave, for the case $P_1 \gg P_2$ with pump and signal powers maintained in a low power regime. We show that an accurate description of the FWM process in the low power regime can only be obtained by including the nonlinear contribution and polarization dependent effects in the scalar FWM theory. The theoretical results were validated experimentally through the measurement of the optical power generated in the idler wave through the FWM process in a DSF. We verify the possibility of efficient generation of idler wave outside of the zero-dispersion of the fiber and with pump and signal fields far apart. We also show experimentally that exist a transition region over which the pump and signal fields go from an almost co-polarized situation to a decorrelated state of polarization. In order to describe the influence of the polarization effects on the evolution of the idler power, we introduced the effective nonlinear parameter, $\gamma_{\text{eff}}(\Delta\lambda)$. We found that the $\gamma_{\text{eff}}(\Delta\lambda)$ varies as an hyperbolic secant with the wavelength separation between pump and signal. This result was obtained for a single sample of a DSF, a sample that we had available in our laboratory. Although we believe that this result can be generalized for other fibers, this should be validated in further studies. We show that if we use the FWM process to measure the fiber nonlinear parameter, what we obtain is the effective nonlinear parameter of the fiber, which is dependent of the wavelength separation between pump and signal fields.

Acknowledgment

The authors would like to thank Prof. G. P. Agrawal for the useful discussion about nonlinear and polarization dependent effects in optical fibers. The authors also thank the reviewers for their suggestions and constructive comments, providing the opportunity to improve the paper.

References

[1] G. P. Agrawal, *Nonlinear Fiber Optics*, 3rd ed. San Diego, CA: Academic, 2001.

[2] G. P. Agrawal, *Applications of Nonlinear Fiber Optics*. San Diego, CA: Academic, 2001.

[3] B. P. Pal, "Fiber-optic parametric amplifiers for lightwave systems," in *Guided Wave Optical Components and Devices*. San Diego, CA: Academic, 2005.

[4] R. H. Stolen and J. E. Bjorkholm, "Parametric amplification and frequency conversion in optical fibers," *IEEE J. Quantum Electron.*, vol. 18, no. 7, pp. 1062–1072, Jul. 1982.

[5] J. Hanstyd, P. A. Andrekson, M. Westlund, J. Li, and P. Hedekvist, "Fiber-based optical parametric amplifiers and their applications," *IEEE J. Sel. Topics Quantum Electron.*, vol. 8, no. 3, pp. 506–520, May/Jun. 2002.

[6] K. Inoue and H. Toba, "Wavelength conversion experiment using fiber four-wave mixing," *IEEE Photon. Technol. Lett.*, vol. 4, pp. 69–72, 1992.

[7] K. Inoue, "Tunable and selective wavelength conversion using fiber four-wave mixing with two pump lights," *IEEE Photon. Technol. Lett.*, vol. 6, no. 12, pp. 1451–1453, Dec. 1994.

[8] Q. Lin and G. P. Agrawal, "Effects of polarization-mode dispersion on fiber-based parametric amplification and wavelength conversion," *Opt. Lett.*, vol. 29, no. 10, pp. 1114–1116, 2004.

[9] P. Antunes, P. S. André, and A. N. Pinto, "Single-photon source by means of four-wave mixing inside a dispersion-shifted optical fiber," in *Proc. Frontiers Opt.*, Oct. 2006, Paper FMJ3.

[10] M. Fiorentino, P. L. Voss, J. E. Sharping, and P. Kumar, "All-fiber photon-pair source for quantum communications," *IEEE Photon. Technol. Lett.*, vol. 14, no. 7, pp. 983–985, Jul. 2002.

[11] X. Li, J. Chen, P. Voss, J. Sharping, and P. Kumar, "All-fiber photon-pair source for quantum communications: Improved generation of correlated photons," *Opt. Expr.*, vol. 12, no. 16, pp. 3737–3744, 2004.

[12] R. H. Stolen, J. E. Bjorkholm, and A. Ashkin, "Phase-matched three-wave mixing in silica fiber optical waveguides," *Appl. Phys. Lett.*, vol. 27, pp. 308–310, 1974.

[13] Q. Lin and G. P. Agrawal, "Vector theory of four wave mixing: Polarization effects in fiber optic parametric amplifiers," *J. Opt. Soc. Amer. B*, vol. 21, pp. 1216–1224, 2004.

[14] Q. Lin, F. Yaman, and G. P. Agrawal, "Photon-pair generation in optical fibers through four-wave mixing: Role of raman scattering and pump polarization," *Phys. Rev. A*, vol. 75, p. 023803, 2007.

[15] E. A. Golovchenko and A. N. Pilipetskii, "Undified analysis of four-photon mixing, modulation instability, and stimulated raman scattering under various polarization conditions in fibers," *J. Opt. Soc. Amer. B*, vol. 11, pp. 92–101, 1994.

[16] C. J. McKinstrie, A. V. Kanaev, and H. Kogelnik, "Nonlinear dynamics associated with a model of vector four-wave mixing," *Opt. Expr.*, vol. 13, pp. 1580–1597, 2005.

[17] C. J. McKinstrie, H. Kogelnik, R. M. Jopson, S. Radic, and A. V. Kanaev, "Four-wave mixing in fibers with random birefringence," *Opt. Expr.*, vol. 12, pp. 2033–2055, 2004.

[18] K. Inoue, "Four-wave mixing in an optical fiber in the zero-dispersion wavelength region," *J. Lightw. Technol.*, vol. 10, no. 11, pp. 1553–1561, Nov. 1992.

[19] K. Washio, K. Inoue, and S. Kishida, "Efficient large-frequency-shifted three-wave mixing in low dispersion wavelength region in single-mode optical fiber," *Electron. Lett.*, vol. 16, no. 17, pp. 658–660, 1980.

[20] C. Lin, W. A. Reed, A. D. Pearson, and H. T. Shang, "Phase matching in the minimum-chromatic-dispersion region of single-mode fibers for stimulated four-photon mixing," *Opt. Lett.*, vol. 6, no. 10, pp. 493–495, 1981.

[21] C. Lin, W. A. Reed, A. D. Pearson, H.-T. Shang, and P. F. Glodis, "Designing single-mode fibres for near-ir(1.1–1.7 μm) frequency generation by phase-matched four-photon mixing in the minimum chromatic dispersion region," *Electron. Lett.*, vol. 18, no. 2, pp. 87–89, 1982.

[22] S. J. Jung, J. Y. Lee, and D. Y. Kim, "Novel phase-matching condition for a four wave mixing experiment in an optical fiber," *Opt. Expr.*, vol. 14, pp. 35–43, 2005.

[23] W. Tittel and G. Weihs, "Photonic entanglement for fundamental tests and quantum communication," *Quantum Inf. Comput.*, vol. 1, pp. 3–56, 2001.

[24] T. Jennewein, C. Simon, G. Weihs, H. Weinfurter, and A. Zeilinger, "Quantum cryptography with entangled photons," *Phys. Rev. Lett.*, vol. 84, no. 20, pp. 4729–4732, 2000.

[25] L. J. Wang, C. K. Hong, and S. R. Friberg, "Generation of correlated photons via four-wave mixing in optical fibrer," *J. Opt. B: Quantum Semiclass.*, vol. 3, pp. 346–352, 2001.

[26] H. Takesue and K. Inoue, "Generation of polarization-entangled photon pairs and violation of Bell's inequality using spontaneous four-wave mixing in a fiber loop," *Phys. Rev. A*, vol. 70, p. 031802, 2004.

[27] H. Takesue and K. Inoue, "Generation of 1.5- μm band time-bin entanglement using spontaneous fiber four-wave mixing and planar lightwave circuit interferometers," *Phys. Rev. A*, vol. 72, p. 041804, 2005.

[28] id 200 Single-Photon Detector Module, id Quantique [Online]. Available: http://www.idquantique.com/products/files/id200-operating.pdf

[29] A. Karlsson, M. Bourennane, G. Ribordy, H. Zbinden, J. Brendel, J. Rarity, and P. Tapster, "A single-photon counter for long-haul telecom," *IEEE Circuits Devices Mag.*, vol. 15, no. 6, pp. 34–40, 1999.

[30] A. Trifonov, D. Subacius, A. Berzanskis, and A. Zavriyev, "Single photon counting at telecom wavelength and quantum key distribution," *J. Mod. Opt.*, vol. 51, no. 9–10, pp. 1399–1415, 2004.

[31] M. Liu, C. Hu, X. Bai, X. Guo, J. C. Campbell, Z. Pan, and M. M. Tashima, "High-performance InGaAs/InP single-photon avalanche photodiode," *IEEE J. Sel. Topics Quantum Electron.*, vol. 13, no. 4, pp. 887–894, Jul./Aug. 2007.

[32] K. O. Hill, D. C. Johnson, B. S. Kawasaki, and R. I. MacDonald, "CW three-wave mixing in single-mode optical fibers," *J. Appl. Phys.*, vol. 49, pp. 5098–5106, 1978.

[33] N. Shibata, R. P. Braun, and R. G. Waarts, "Phase-mismatch dependence of efficiency of wave generation through four-wave mixing in a single-mode optical fiber," *IEEE J. Quantum Electron.*, vol. 23, no. 7, pp. 1205–1210, Jul. 1987.
[34] J. R. Thompson and R. Roy, "Multiple four-wave mixing process in an optical fiber," *Opt. Lett.*, vol. 16, no. 8, pp. 557–559, 1991.
[35] J. R. Thompson and R. Roy, "Nonlinear dynamics of multiple four-wave mixing processes in a single-mode fiber," *Phys. Rev. A*, vol. 43, no. 9, pp. 4987–4996, 1991.
[36] X. Liu, X. Zhou, and C. Lu, "Multiple four-wave mixing self-stability in optical fibers," *Phys. Rev. A*, vol. 72, p. 013811, 2005.
[37] K. Kikuchi and Chaloemphon, "Design of highly efficient four-wave mixing devices using optical fibers," *IEEE Photon. Technol. Lett.*, vol. 6, no. 8, pp. 992–994, Aug. 1994.
[38] R. W. McKerracher, J. L. Blows, and C. M. de Sterke, "Wavelength conversion bandwidth in fiber based optical parametric amplifiers," *Opt. Expr.*, vol. 11, no. 9, pp. 1002–1007, 2003.
[39] M. Farahmand and M. de Sterke, "Parametric amplification in presence of dispersion fluctuations," *Opt. Expr.*, vol. 12, no. 1, pp. 136–142, 2004.
[40] M. Karlsson, "Four-wave mixing in fibers with randomly varying zero-dispersion wavelength," *J. Opt. Soc. Amer. B*, vol. 15, no. 8, pp. 2269–2275, 1998.
[41] P. K. A. Wai, C. R. Menyuk, and H. H. Chen, "Stability of solitons in randomly varying birefringent fibers," *Opt. Lett.*, vol. 16, no. 16, pp. 1231–1233, 1991.
[42] Q. Lin and G. P. Agrawal, "Polarization mode dispersion-induced fluctuations during raman amplifications in optical fibers," *Opt. Lett.*, vol. 27, pp. 2194–2196, 2002.
[43] S. G. E. , Jr., L. F. Mollenauer, J. P. Gordon, and N. S. Bergano, "Polarization multiplexing with solitons," *J. Lightw. Technol.*, vol. 10, no. 1, pp. 28–35, Jan. 1992.
[44] Q. Lin and G. P. Agrawal, "Impact of polarization-mode dispersion on measurement of zero-dispersion wavelength through four-wave mixing," *IEEE Photon. Technol. Lett.*, vol. 15, no. 12, pp. 1719–1721, Dec. 2003.
[45] Q. Lin and G. P. Agrawal, "Effects of polarization-mode dispersion on fiber-based parametric amplification and wavelength conversion," *Opt. Lett.*, vol. 29, pp. 1114–1116, 2004.
[46] C. D. Poole and R. E. Wagner, "Phenomenological approach to polarisation dispersion in long single-mode fibres," *Electron. Lett.*, vol. 22, pp. 1029–1031, 1986.
[47] R. M. Jopson, L. E. Nelson, and H. Kogelnik, "Measurement of second-order polarization-mode dispersion vectors in optical fibers," *IEEE Photon. Technol. Lett.*, vol. 11, no. 9, pp. 1153–1155, Sep. 1999.

Nuno Alexandre Silva was born in Fafe, Portugal, in 1981. He received the physics degree from the University of Minho, Portugal, in 2006.

He is currently working as a Researcher in the Optics Communications group of the Institute of Telecommunications, Aveiro. His current main interests of research are nonlinear fiber optics, polarization and quantum effects in optical fibers.

Nelson Jesus Muga was born in Mogadouro, Portugal, in 1980. He received the physics degree from the University of Porto, Portugal, in 2002, and the M.S. degree in applied physics from the University of Aveiro, Portugal, in 2006. He is currently pursuing the Ph.D. degree at the University of Aveiro, Portugal.

His current main research interests are nonlinear and polarization effects in optical fibers.

Armando Nolasco Pinto (M'99–SM'07) was born in Oliveira do Bairro, Portugal, in 1971. He graduated in electronic and telecommunications engineering in 1994, and received the Ph.D. degree in electrical engineering in 1999, both from the University of Aveiro, Aveiro, Portugal. In 1995 and 1996, as part of his Ph.D. studies, he worked with Prof. Govind Agrawal at The Institute of Optics, University of Rochester, Rochester, NY.

In 2000, he became an Assistant Professor at the Electrical, Telecommunications and Informatics Department, University of Aveiro, and a Researcher at the Institute of Telecommunications, Aveiro. During the academic year of 2006–2007 he was a Visiting Professor at the Institute of Optics, University of Rochester, Rochester, NY. At present, he leads a research group at the Institute of Telecommunications focus on high-speed optical communication systems and networks. He has published more than 100 scientific papers in international journals and conferences.

Dr. Pinto is a member of the Optical Society of America (OSA).